

Adsorption of Gases on $\text{Ti}_3\text{C}_2\text{T}_x$ MXene: Implications from X-ray Photoelectron Spectroscopy

*Lars-Åke Näslund, * Esko Kokkonen, and Martin Magnuson*

L.-Å. Näslund, M. Magnuson

Thin Film Physics Division, Department of Physics, Chemistry, and Biology (IFM),
Linköping University, SE-581 83 Linköping, Sweden

E-mail: lars-ake.naslund@liu.se

E. Kokkonen

MAX IV Laboratory, Lund University, SE-221 00 Lund, Sweden

Keywords: adsorption, H_2 , CO_2 , H_2O , X-ray photoelectron spectroscopy

One of the most explored MXenes is the $\text{Ti}_3\text{C}_2\text{T}_x$, where T_x is designated to inherently formed termination species. Among many applications, $\text{Ti}_3\text{C}_2\text{T}_x$ is an excellent material for energy storage, energy converting, and CO_2 -capturing devices. However, active sites for adsorption and surface reactions on the $\text{Ti}_3\text{C}_2\text{T}_x$ -surface are still open questions to explore, which have implications for preparation methods when to obtain correct and optimized surface requirements. Here we use X-ray photoelectron spectroscopy to study adsorption of common gas molecules such as H_2 , CO_2 , and H_2O , which all might be present in energy storage, energy converting, and CO_2 -capturing devices based on 2D flakes of $\text{Ti}_3\text{C}_2\text{T}_x$. The study shows that H_2O , with a strong bonding to the Ti-Ti bridge-sites, can be considered as a termination species. An H_2O terminated $\text{Ti}_3\text{C}_2\text{T}_x$ -surface restricts the CO_2 adsorption to the Ti on-top sites and reduces the ability to store positive ions, such as Li^+ and Na^+ . On the other hand, an H_2O terminated $\text{Ti}_3\text{C}_2\text{T}_x$ -surface shows the capability to split water. The study further shows that H_2 has the ability to remove F at moderate temperatures. The results from this study have implications for correct selection of MXene preparations and the environment around the MXene in different implementations.

1. Introduction

Transition metal carbides or nitrides known as MXenes are two-dimensional (2D) materials that can be engineered for a variety of applications with fine-tuned properties.^[1,2] MXenes consist of a transition metal (M), carbon or nitrogen (X), and termination species (T_x) forming a layered compound denoted $M_{n+1}X_nT_x$. One of the most studied MXenes is $Ti_3C_2T_x$, which consists of three Ti-monolayers and two C-monolayers stacked in an alternated sequence where the first and the last Ti-monolayers form surfaces terminated by T_x . The inherently formed T_x on the Ti_3C_2 -surfaces have in rigorous X-ray photoelectron spectroscopy (XPS) and ultraviolet photoelectron spectroscopy (UPS) studies been identified to be fluorine (F) and oxygen (O).^[3-6]

While termination species are essential for the formation of the delaminated Ti_3C_2 -layers, adsorbates are atoms and molecules that exist on the $Ti_3C_2T_x$ -surface in equilibrium with the surrounding at specific conditions. This distinction is made because the termination species are remarkably stable and therefore difficult to remove or replace^[7] while adsorbates exist on the surface only when the correct conditions are fulfilled.

Nevertheless, F can be removed with a heat treatment^[3] and a recent in situ study using environmental transmission electron microscopy, electron energy loss spectroscopy, and mass spectroscopy showed that hydrogen (H_2) exposure at 700 °C can remove the termination species O by forming water (H_2O) that desorbs from the Ti_3C_2 -surface.^[8] Without termination species, the Ti_3C_2 -surface became an effective carbon dioxide (CO_2) capture material without competition from nitrogen (N_2) adsorption.^[8] Hence, termination free $Ti_3C_2T_x$ as a carbon-capturing material is proven to have promising properties, such as chemical and thermal stability, CO_2/N_2 selectivity, and effective adsorption of CO_2 .^[8]

Termination species are also essential in intercalation processes where they act as anchor points of ions, such as Li^+ and Na^+ , in energy storage devices or activates the MXene-surface in electrochemical energy conversion applications.^[5,9]

Although successful removals of the termination species F and O and subsequent adsorption of CO₂ have been accomplished,^[8] there is very little knowledge about the interaction between Ti₃C₂T_x and common gas molecules such as H₂, CO₂, and H₂O. Here, we employ high-resolution XPS to study the adsorption of H₂, CO₂, and H₂O. Since XPS provides element-specific information on the electronic structure of the probed atoms, it is possible to gain information about the chemical environment around the adsorbed molecules. Hence, XPS is a suitable technique to study the complex interactions between H₂, CO₂, and H₂O on the Ti₃C₂T_x-surface, which affect the efficiency/quality of the Ti₃C₂T_x as a catalyst, carbon capturing material, energy conversion material, gas sensing material, or any other application involving adsorption of gas molecules on the Ti₃C₂T_x-surface with different termination species.

2. Experimental Section

2.1. Sample Preparation

Ti₃C₂T_x flakes were produced from powder of Ti₃AlC₂, which were made from TiC (Alfa Aesar, 98+%), Ti (Alfa Aesar, 98+%), and Al (Alfa Aesar, 98+%) in a 1:1:2 molar ratios. The formed Ti₃AlC₂ powder was exposed to an etching process involving 10 ml aqueous solution of 12 M HCl (Fisher, technical grade) and 2.3 M LiF (Alfa Aesar, 98+%) at 35 °C for 24 h. The produced Ti₃C₂T_x flakes were contained in a deionized water suspension with a concentration of 1 mg ml⁻¹, which was filtered through a nanopolypropylene membrane (3501 Coated PP, 0.064 μm pore size, Celgard, USA) to make a freestanding film. The obtained Ti₃C₂T_x foil was thereafter stored in argon (Ar) atmosphere. Further details about the sample preparation have been presented previously.^[5]

2.2. Sample Mounting and Heating

A piece of the Ti₃C₂T_x freestanding film with the size of ca. 20 x 10 mm² was placed on a sample holder with two stainless steel clips. A chromel/alumel thermocouple was spot welded onto the sample holder between the clips under the Ti₃C₂T_x freestanding film. The sample holder system enabled monitoring of the sample temperature, both in the ultra-high vacuum (UHV) chamber and in the ambient pressure cell. In addition to the thermocouple reading, the sample temperature was also measured using a Cyclops 160L pyrometer from Land Ametek when the sample heating was performed in the UHV chamber. The sample heating in the UHV chamber was obtained through

electron bombardment on the backside of the sample holder and controlled through a bias over the sample holder. In the ambient pressure cell, the sample was heated using a resistive heater located behind the sample holder. No Ar⁺ sputtering was performed.

2.3. Gas Exposure Experiments

The Ti₃C₂T_x freestanding film was exposed to different gases in an ambient pressure gas cell. H₂ and CO₂ gases (purity 99.99% or better), obtained from Air Liquide Gas AB, were used without any extra purification. H₂O vapor was obtained from deionized H₂O, which was cleaned with three freeze-pump-thaw cycles to remove any dissolved gases. The pressure inside the cell was monitored using a gas independent manometer located on the outlet line of the cell. After gas exposure the ambient pressure cell was evacuated before XPS data acquisition.

2.4. XPS Measurements

The XPS measurements were performed using a SPECS Phoibos 150 NAP electron energy analyzer installed on the ambient pressure XPS endstation at the SPECIES beamline^[10,11] at the synchrotron radiation facility MAX IV Laboratory in Lund, Sweden. The photon beam from the beamline, with the photon energy of 780 eV, impinged onto the sample at an angle of 57°, with respect to the surface normal, and provided an X-ray spot size of approximately 100 x 100 μm². The photoelectrons were entering the electron energy analyzer with an acceptance angle of ±22° from the sample surface normal. The core level XPS spectra were recorded with a step size of 0.05 eV and pass energy of 50 eV, which provided an overall energy resolution better than 0.25 eV. The binding energy scale of all XPS spectra was calibrated using the sample Fermi-edge (E_f), which was set to a binding energy of 0.00 ±0.02 eV. The XPS spectra were also normalized at the background on the low binding energy side of the main peak/peaks.

2.5. XPS Spectra Curve Fittings

The background contribution in each XPS spectrum was removed using a Shirley function before curve fitting of the spectrum.^[6,12] The background subtractions and the curve fittings of the F 1s, O 1s, Ti 2p, and C 1s XPS spectra were performed using Igor Pro version 6.22A from WaveMetrics, which is a technical graphing and data analysis software for scientists and engineers.^[13] The peak fitting procedure was

based on first principles thinking as described in a previous work.^[6] The XPS spectra were curve fitted using convoluted Lorentzian- and Gaussian functions, aka Voigt functions, with tails toward higher binding energies.^[6] The binding energy positions of the Voigt functions might differ slightly (± 0.05 eV) from previous work^[3,4,6] because of minor deviations in the kinetic energy measurements of the photoelectrons.

3. Results and Discussion

3.1. XPS Spectra comparison

3.1.1. XPS Spectra of $Ti_3C_2T_x$

Figure 1 displays the XPS spectra of the $Ti_3C_2T_x$ freestanding film obtained before and after a heat treatment at 670 °C for 30 min in vacuum with the base pressures below 1×10^{-9} mBar. The XPS spectra of $Ti_3C_2T_x$ have been analyzed in detail^[3-6] and since the XPS spectra in Figure 1 show resemblance with those presented in the previous works the interpretation is straightforward (according to Refs.^[3,4,6]).

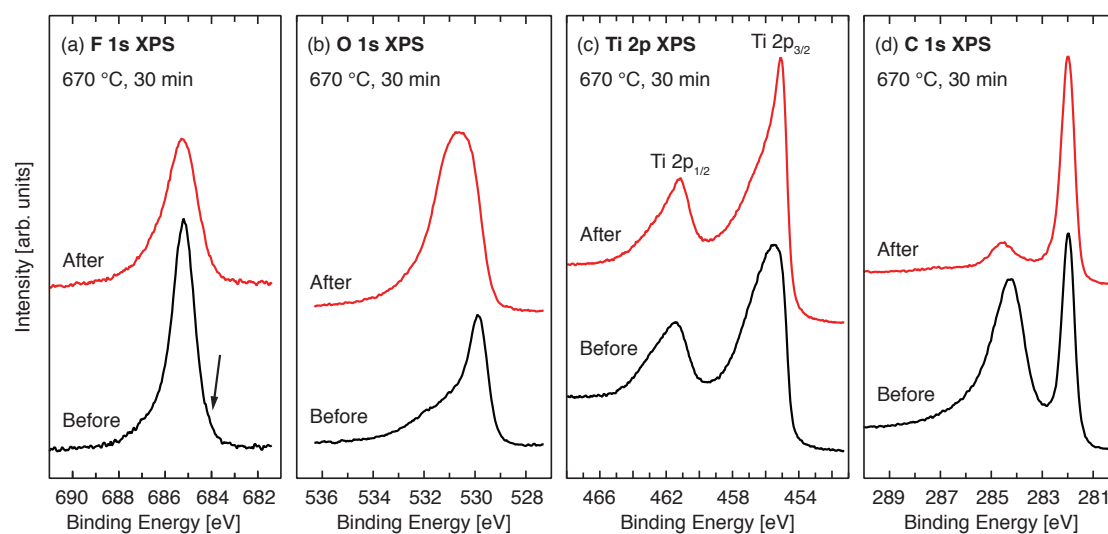


Figure 1. XPS spectra of the freestanding $Ti_3C_2T_x$ film for the core levels (a) F 1s, (b) O 1s, (c) Ti 2p, and (d) C 1s. The XPS spectra were obtained before and after a 670 °C heat treatment for 30 min. The arrow in (a) is pointing on a barely observable shoulder. The photon energy was 780 eV.

The shape of the F 1s XPS peak at 685.2 eV has, in a previous work, been revealed to be two features located at 684.5 and 685.3 eV assigned to F on the face-centered

cubic (fcc) site.^[3,4,6] The former originates from domains with only F and the latter from F that shares Ti-bonding with O.^[6] An almost imperceptible shoulder on the low binding energy side of the F 1s XPS spectrum in Figure 1(a) (indicated by an arrow) suggests that the $Ti_3C_2T_x$ sample also in this study has domains with only F, although in very small amount. The O 1s XPS spectrum obtained before the heat treatment, displayed in Figure 1(b), is dominated by a feature at 529.8 eV, which originates from O bonded to two Ti atoms in a bridge position.^[3-6] The shoulder on the high binding energy side originates from residual Al_2O_3 and from O on the fcc-site.^[3-6] The Ti 2p XPS spectrum obtained before the heat treatment, displayed in Figure 1(c), shows the spin orbit splitting with the intensity for Ti 2p_{3/2} in the 455.5-457.7 eV range and for Ti 2p_{1/2} in the 461.9-464.1 eV range. The absence of features in the 457.7-461.9 range confirms that the $Ti_3C_2T_x$ sample is free from TiO_2 and other titanium oxide components.^[3,4,6] The C 1s XPS spectrum obtained before the heat treatment, displayed in Figure 1(d), shows a sharp carbide peak at 282.0 eV and a relatively high graphite-like peak at 284.2 eV. The carbide peak with the binding energy position at 282.0 eV is a reliable indication of a successful formation of $Ti_3C_2T_x$.^[14] The graphite-like peak at 284.2 eV^[15] indicates, on the other hand, an excessive etching procedure that broke a large number of Ti-C bonds in the Ti_3C_2 -layers in the process of transforming MAX-phase into MXene.

3.1.2. $Ti_3C_2T_x$ Heat Treatment

The peak at 284.2 eV in the C 1s XPS spectrum before the heat treatment shown in Figure 1 indicates a significant amount of graphite-like carbon in the sample.^[15] However, the heating process removed most of the graphite-like carbon and thus the graphite-like carbon suggests to have been formed as an overlayer on the freestanding $Ti_3C_2T_x$ film in the final filtering step (see the Experimental Section). The difference in heat expansion between the $Ti_3C_2T_x$ and the graphite-like carbon is probably the reason why the graphite-like carbon is removed in the heating process.

The F 1s intensity and the shape of the Ti 2p XPS spectrum in Figure 1(a) and 1(c) show that the amount of F has been reduced in the heating process, as observed in a previous work.^[3] A drawback with the $Ti_3C_2T_x$ freestanding film is that during the heat treatment the film expands and becomes buckled leading to poor contact between the $Ti_3C_2T_x$ sample and the sample holder. Consequently, while the thermocouple

reading showed a much higher temperature on the sample holder, the pyrometer reading showed a sample temperature of only 670 °C (the temperature reading for the pyrometer when pointing towards the sample holder agreed with the thermocouple reading). It was therefore not possible to reach the temperatures needed to remove F completely,^[3] which was the intention. Further, the O 1s XPS spectrum of the heat-treated $Ti_3C_2T_x$ in Figure 1(b) shows an increased intensity compared with the as-prepared $Ti_3C_2T_x$. Since the integrated XPS intensity is proportional to the amount of the probed element, this finding indicates adsorption of oxygen containing species during the heat treatment. Based on the fact that the heat treatment was performed in UHV conditions, the source of the oxygen containing species must be in the interior of the sample. Hence, the heat treatment shows that the intercalated species that bind the 2D flakes together in the $Ti_3C_2T_x$ freestanding film consist of oxygen containing species.

Wet etching using an aqueous solution containing high concentration of HCl will leave some Cl on the surface of the produced $Ti_3C_2T_x$ freestanding film, as shown in **Figure 2**. However, the heat treatment at 670 °C for 30 min removed the Cl almost completely. Chlorine as an inherent termination species on $Ti_3C_2T_x$ can therefore be questioned. As a matter of fact, the Cl was removed together with the graphite-like carbon, which suggest that most of the Cl was adsorbed on the graphite-like carbon.

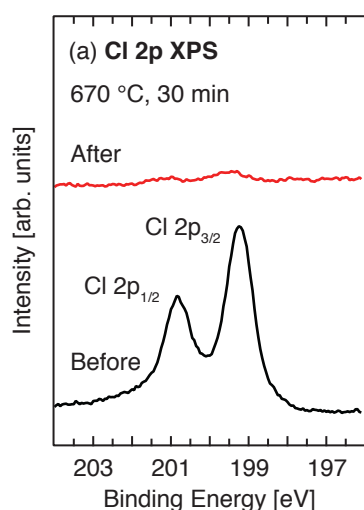


Figure 2. XPS spectra of the freestanding $Ti_3C_2T_x$ film for the core level Cl 2p. The XPS spectra were obtained before and after a 670 °C heat treatment for 30 min. The photon energy was 780 eV.

3.1.3. H₂ Gas Exposure

The sample was transferred into an ambient pressure gas cell for H₂ gas exposure. **Figure 3** shows the XPS spectra of the Ti₃C₂T_x freestanding film before and after 3 mbar H₂ gas exposure for 3 h, where the first 2.5 h were at a sample holder temperature of 450 °C and the last 0.5 h without heating, i.e., during the cool-down of the sample. Figure 3(a) shows that H₂ effectively removes F as the F 1s XPS peak at 685.2 eV has disappeared completely. It is also clear from Figure 3(b) that the O 1s XPS intensity has increased and, in addition, has shifted by -0.5 eV, i.e., from a peak maximum at 530.6 eV to 530.1 eV. Two new features have also appeared in the Ti 2p XPS spectrum, at 458.2 eV and 464.2 eV, as indicated with the arrows in Figure 3(c). The Ti 2p_{3/2} XPS peak at 455.1 eV remains, although with slightly reduced intensity. Thorough curve fittings of all O 1s and Ti 2p XPS spectra, as presented in section 3.2, are needed before all the observed binding energy shifts and appeared features at different treatments can be interpreted.

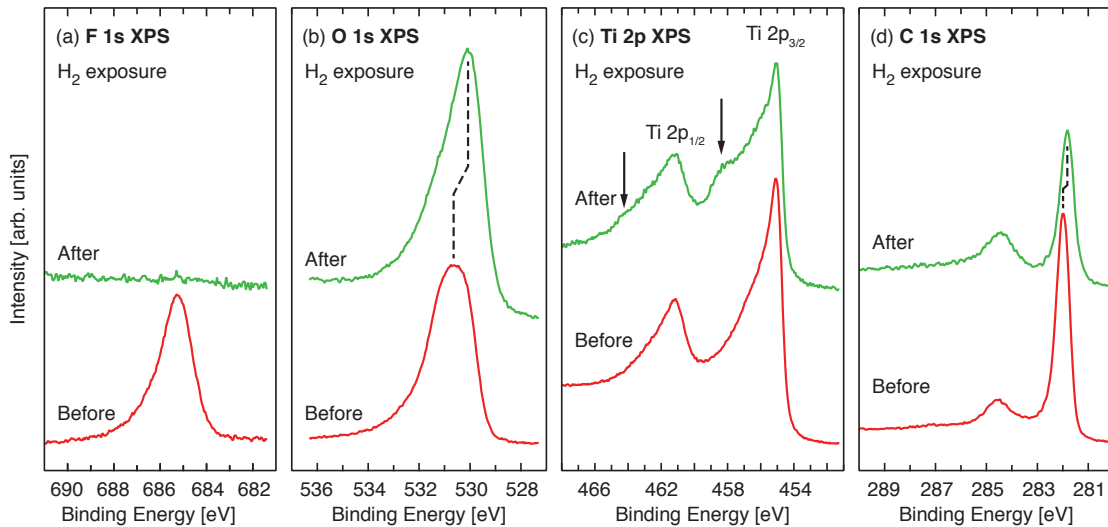


Figure 3. XPS spectra of the freestanding Ti₃C₂T_x film for the core levels (a) F 1s, (b) O 1s, (c) Ti 2p, and (d) C 1s. The XPS spectra were obtained before and after 3 mbar H₂ gas exposure for 3 h. The photon energy was 780 eV.

The C 1s XPS peak in Figure 3(d) shows a shift toward lower binding energies by -0.2 eV after the H₂ gas exposure, suggesting that the hydrogen atoms contribute charge to the two C layers in the Ti₃C₂T_x crystal structure upon H adsorption. In

addition, the negative shift of the whole carbide peak infers a non-localized distribution of the extra electrons in the two C layers. The intensity of the carbide peak has remarkably been reduced after the H₂ exposure.

3.1.4. CO₂ Gas Exposure 1

After the H₂ exposure the sample was exposed to CO₂. **Figure 4** shows the XPS spectra obtained before and after the H saturated Ti₃C₂T_x-surface was exposed to 3.5 mbar CO₂ for 1.5 h at 250 °C. The XPS spectra show only minor changes. Both the O 1s and C 1s XPS peaks shift less than 0.1 eV toward higher binding energies, which suggest a slight decrease of the H coverage. Whether the H coverage reduction is because of the CO₂ exposure, the heat treatment at 250 °C, or by local variations cannot be settled by the presented XPS data solely. However, the freestanding film consists of a large number of 2D flakes, which introduce small local variations on the Ti₃C₂T_x-surface in terms of, e.g., geometry and thermal conductivity. New measurement spots on the Ti₃C₂T_x sample, which is inevitable after every gas dosing, is therefore expected to show small variations in the XPS spectra. The local geometry might also cause fluctuations in H coverage on the Ti₃C₂T_x-surface.

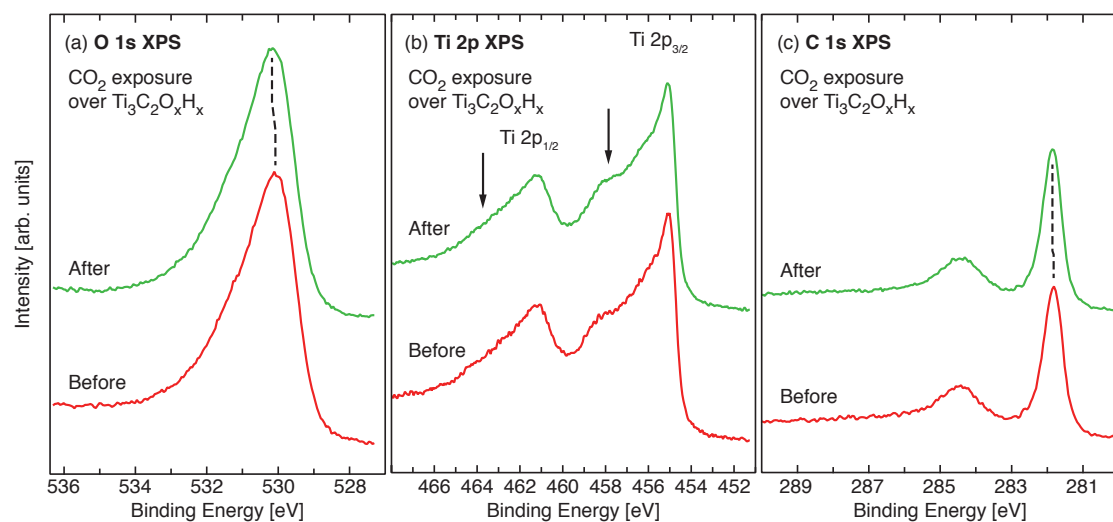


Figure 4. XPS spectra of the freestanding Ti₃C₂O_xH_y film for the core levels (a) O 1s, (b) Ti 2p, and (c) C 1s. The XPS spectra were obtained before and after 3.5 mbar CO₂ gas exposure for 1.5 h. The photon energy was 780 eV.

3.1.5. CO₂ Gas Exposure 2

After removing the adsorbed H through a heat treatment at 450 °C for 35 min the sample was exposed to 11 mbar CO₂ at 450 °C for 1 h. **Figure 5** shows the XPS spectra of the Ti₃C₂T_x before and after the CO₂ exposure. The dotted spectrum in Figure 5(b) is the Ti 2p spectrum after the heat treatment of Ti₃C₂T_x at 650 °C but before the H₂ gas exposure, which is shown in Figure 1. The direct comparison of the Ti 2p spectra shows that the 35 min heat treatment at 450 °C was not enough to remove all H from the Ti₃C₂T_x-surface. Also the XPS peak positions of O 1s and C 1s, which have binding energies 530.5 and 281.9 eV, respectively, indicate that some amount of H remains.

Nevertheless, after the CO₂ exposure there are clear changes in the O 1s, Ti 2p, and C 1s XPS spectra indicating CO₂ adsorption. The O 1s XPS peak shows an increased intensity and a -0.2 eV binding energy shift to 530.3 eV, compared to the binding energy 530.5 eV before the CO₂ gas exposure. The Ti 2p XPS spectrum shows two additional peaks that appear at 458.7 and 464.5 eV. The C 1s XPS spectrum shows an increased intensity at 284.6 eV and a slight shift toward lower binding energies for the carbide peak. The increased intensities for the O 1s XPS peak around 530.3 eV and for C 1s XPS peak around 284.6 eV indicate CO₂ adsorption.^[16] In addition, the absence of features in the binding energy region 286-290 eV in the C 1s spectra in Figure 5 infer that there are no significant amounts of alcohol, carboxyl nor carbonate formed on the Ti₃C₂T_x-surface upon CO₂ adsorption.^[4,17,18] (There might be a weak feature at 287 eV suggesting a small amount of alcohol compounds present in a few C 1s XPS spectra, e.g., after first heat treatment in Figure 1 and after CO₂ exposure in Figure 5.)

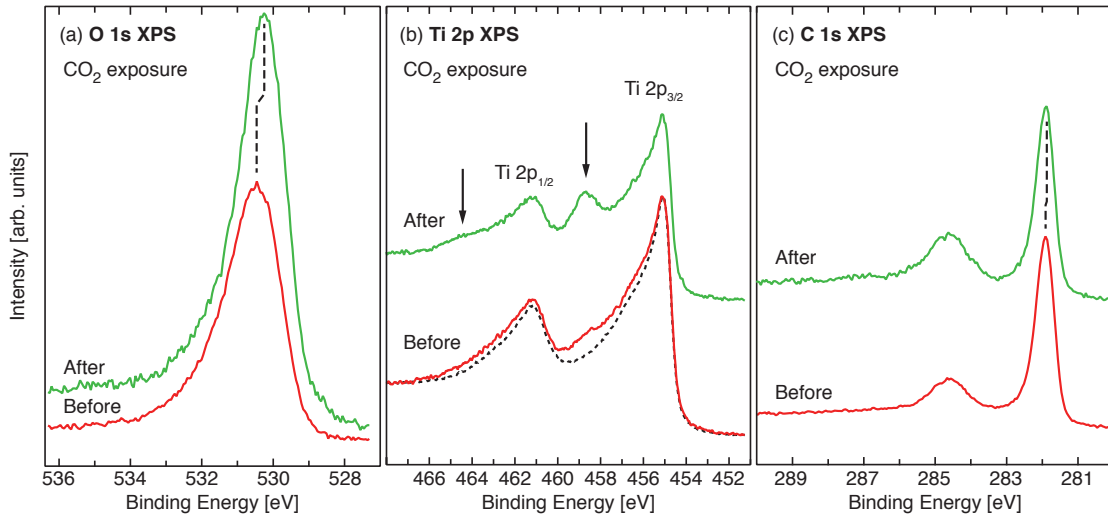


Figure 5. XPS spectra of the freestanding $\text{Ti}_3\text{C}_2\text{T}_x$ film for the core levels (a) O 1s, (b) Ti 2p, and (c) C 1s. The XPS spectra were obtained before and after 11 mbar CO_2 gas exposure for 1.0 h. The photon energy was 780 eV.

3.1.6. H_2O Gas Exposure

Figure 6 shows that the heat treatment at 650 °C for 1 h removed almost all adsorbed species on the $\text{Ti}_3\text{C}_2\text{T}_x$ -surface. A comparison with the Ti 2p XPS spectrum of the sample before all the gas exposure experiments, presented in Figure 1, suggests that small amounts of H and/or CO_2 remain on the $\text{Ti}_3\text{C}_2\text{T}_x$ -surface. Nevertheless, the carbide peak in the C 1s XPS spectrum is back at 282.0 eV, which is indicative of $\text{Ti}_3\text{C}_2\text{T}_x$ without adsorbates.^[14] A large difference appears in the comparison of the O 1s XPS spectra in Figure 6(a) where the increased integrated intensity infers more oxygen on the $\text{Ti}_3\text{C}_2\text{T}_x$ -surface after the H_2 and CO_2 exposures, including the second and third heat treatments, compared with the $\text{Ti}_3\text{C}_2\text{T}_x$ sample after the first heat treatment shown in Figure 1(b). In addition, the intensity maximum around 531 eV shows increased amount of O on the fcc-site,^[3,4,6] while the shoulder at 530.3 eV suggests the presence of O-containing termination species other than atomic O. The minute shoulder at 532.4 eV indicates presence of residual Al_2O_3 ,^[4,19] which amount can vary depending on selected measuring spot.

Figure 6 shows that the H_2O gas exposure to the $\text{Ti}_3\text{C}_2\text{T}_x$ sample alters the O 1s, Ti 2p and C 1s XPS spectra. After the H_2O exposure the O 1s XPS spectrum shows a redistribution of intensity toward lower binding energies, i.e., the O 1s XPS peak maximum shifts from 531.0 eV to 530.5 eV. The Ti 2p XPS spectrum shows features

at 458.7 and 464.5 eV. The C 1s XPS spectrum shows a small shift of the carbide peak, although it is less than -0.1 eV.

After heat treatment at 700 °C for 5 min the O 1s, Ti 2p and C 1s XPS spectra are almost identical as the corresponding XPS spectra before the H₂O gas exposure.

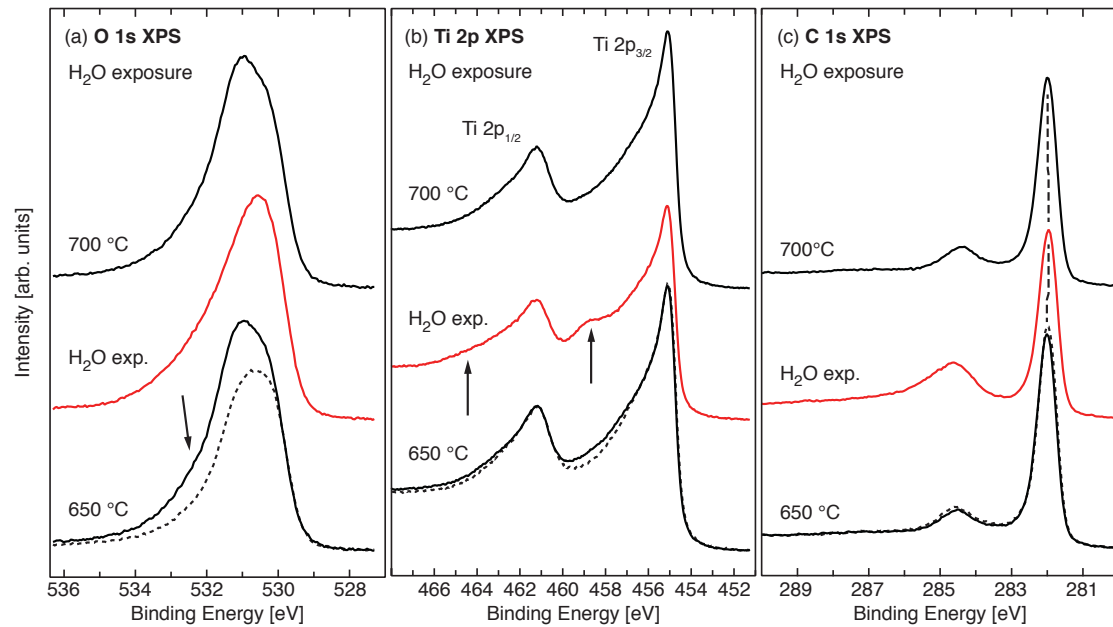


Figure 6. XPS spectra of the freestanding $\text{Ti}_3\text{C}_2\text{T}_x$ film for the core levels (a) O 1s, (b) Ti 2p, and (c) C 1s. The XPS spectra were obtained before and after 3 mbar H₂O gas exposure for 2.0 h and after heat treatment at 700 °C. The arrows in (a) and (b) point at shoulders. The O 1s, Ti 2p, and C 1s XPS spectra with dotted lines are from $\text{Ti}_3\text{C}_2\text{T}_x$ obtained after the first heat treatment at 670 °C presented in Figure 1. The photon energy was 780 eV.

3.2. XPS Spectra Curve Fittings

3.2.1. The As Prepared Sample

Previous studies have concluded that F occupies the fcc-sites while O occupies both fcc-sites and a bridge-site between two Ti atoms.^[3-6] Further, F has precedence over O regarding the fcc-sites, which forces the O to the Ti-Ti bridge-sites when F is present on the $\text{Ti}_3\text{C}_2\text{T}_x$ -surface.^[3] Figure 1 shows that a dominant fraction of O is located on the Ti-Ti bridge-sites and only a small amount of O is located on the fcc-sites. Hence, the F/O ratio is high.

Figure 7 shows curve fittings of the XPS spectra from the sample before the heat treatment. As obtained in previous works, the F 1s XPS spectrum in Figure 7(a) needs two Voigt functions with tails to fit the spectrum. The large feature at 685.2 eV is assigned to F on the fcc-sites that share Ti-bonding with O while the small feature at 684.4 eV is assigned to F in domains with only F.^[3,6] Hence, a Ti atom around an fcc-site occupied with an F can also bond to an O occupying the Ti-Ti bridge-site. The very small intensity of the feature at 684.4 eV suggests that the $\text{Ti}_3\text{C}_2\text{T}_x$ sample in this study is almost saturated by O on the Ti-Ti bridge-sites. The curve fitting on the O 1s XPS spectrum in Figure 7(b) indicates that the amount of O on the fcc-sites was very small, although the green curve at 531.7 eV and the red curve at 531.2 eV show that some O are occupying fcc-sites in domains with F but also on fcc-sites in domains with only O, respectively.^[3,6]

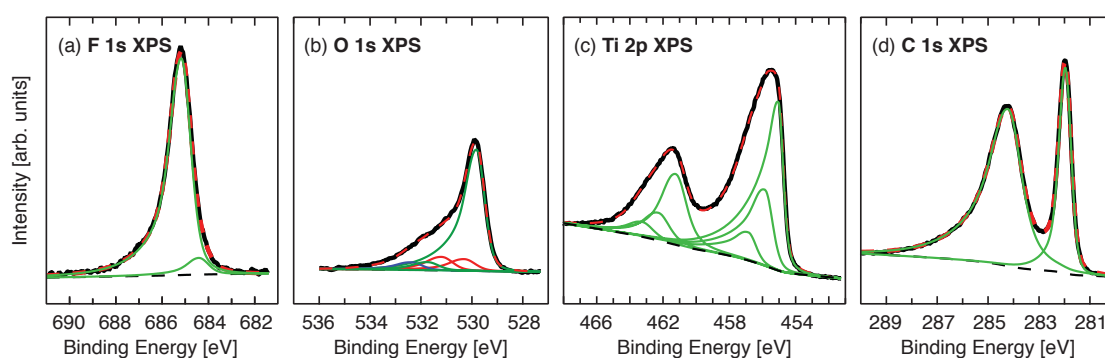


Figure 7. Peak fittings of XPS spectra from the $\text{Ti}_3\text{C}_2\text{T}_x$ film before the heat treatments and gas dosing for the core levels (a) F 1s, (b) O 1s, (c) Ti 2p, and (d) C 1s.

The O on the bridge-site between two surface Ti atoms and the O on the fcc-site provide XPS features at 529.8 eV and 531.7 eV, respectively. Hence, these two different sites for O on the $\text{Ti}_3\text{C}_2\text{T}_x$ -surface – the bridge-site and the fcc-site – lead to binding energies that are separated by 1.9 eV, which may appear large. It is, however, observed also in the classical example of CO adsorption on Pt(111), where CO adsorbs both on top of Pt atoms and between two Pt atoms in a bridge position giving rise to two O 1s peaks with binding energies 532.7 and 531.0 eV, respectively.^[20] Hence, two different sites on the same sample surface can induce a relatively large difference in binding energy even though the adsorbing species is the same. The molecular orbital mixing between the adsorbed atom and the substrate atom depends on the available orbitals and their directions at the occupying site. The bonding

condition will therefore be dissimilar at different sites, which will affect the core hole screening of the probed atom and thus the kinetic energy of the ejected photoelectrons.^[21] The curve fittings of Ti 2p and C 1s XPS spectra in Figure 7(c) and (d) show the same results as in previous works.^[3,4,6]

3.2.2. The Heat Treated Sample

Curve fittings of the XPS spectra after the first heat treatment are presented in **Figure 8**. The reduced amount of F, because of desorption in the heat treatment,^[3] is indicated in the decreased intensity of the fitted Voigt functions in the F 1s spectrum and at 455.8 (462.3) and 456.9 (463.3) eV in the Ti 2p XPS spectrum. The curve fitting of the O 1s XPS spectrum in Figure 8(b) shows also the expected large reduction of the peak at 529.8 eV, the vanishing of the peak at 531.7 eV, and a significant growth of the peak at 531.2 eV, which is indicative of migration of O from the Ti-Ti bridge-sites to domains with only O occupying the fcc-sites.^[3] In addition, there is an unexpected feature at 530.3 eV that dominates the O 1s spectrum after the heat treatment. However, water molecules were intercalated between the $\text{Ti}_3\text{C}_2\text{T}_x$ -flakes when the $\text{Ti}_3\text{C}_2\text{T}_x$ freestanding film was produced, which could be the reason why the flakes do not fall apart thanks to hydrogen bonding between the intercalated H_2O and the O on the Ti-Ti bridge-sites.^[5] During the heat treatment a significant amount of H_2O molecules left the intercalated position and found the vacant Ti-Ti bridge-sites. As observed in Figure 7(b) some H_2O was present on the $\text{Ti}_3\text{C}_2\text{T}_x$ -surface already before the heat treatment, although only in very small amounts since most Ti-Ti bridge-sites were occupied by O that seem to have precedence. During the heat treatment the fcc-sites became vacant and therefore available for O, which migrated from the Ti-Ti bridge position making them available for the intercalated H_2O . That adsorbed H_2O shows higher O 1s binding energy compared with adsorbed O on the same site agrees with a previous work where H_2O and O are coadsorbed on Pt(111).^[22]

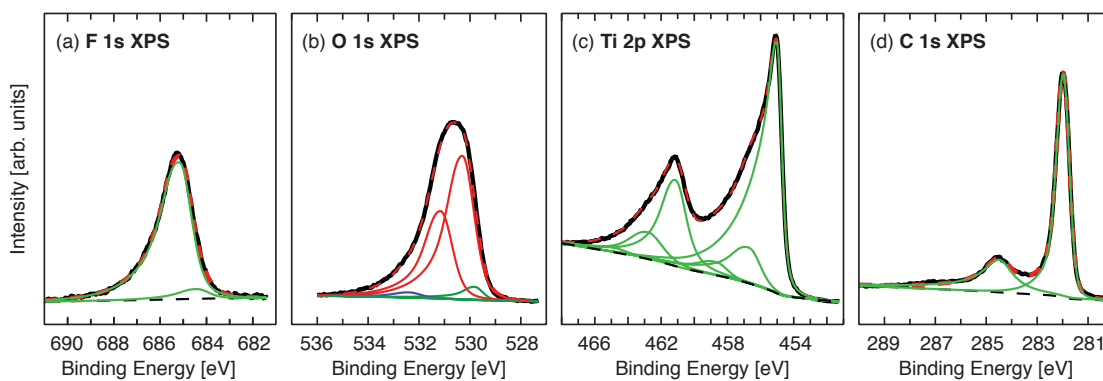


Figure 8. Peak fittings of XPS spectra from the $\text{Ti}_3\text{C}_2\text{T}_x$ film after the heat treatment at $670\text{ }^\circ\text{C}$ for the core levels (a) F 1s, (b) O 1s, (c) Ti 2p, and (d) C 1s.

3.2.3. The H_2 Exposed Sample

Figure 3 showed that the H_2 gas exposure effectively removed F from the $\text{Ti}_3\text{C}_2\text{T}_x$ -surface. In addition, more H_2O diffused from the bulk of the sample to the surface, because the H_2 gas exposure occurred at $450\text{ }^\circ\text{C}$, and the total amount of O-containing species increased until saturation. Curve fitting of the O 1s XPS spectrum is shown in **Figure 9(a)**. Surprisingly, the feature at 531.2 eV , which is assigned to O on the fcc-sites in domains with only O, has decreased and a new feature at 529.8 eV has appeared. Hence, the adsorption of H has forced the O away from the fcc-sites and back into the Ti-Ti bridge-sites. Since the O on the Ti-Ti bridge-sites was coadsorbed with H and H_2O the fitted peak became shifted slightly toward lower binding energies, although only by 0.04 eV (according to the curve fitting).

Furthermore, the Ti 2p XPS spectrum in figure 9(b) shows that two new features, represented by Voigt functions with tails at 456.5 and 458.4 eV , have replaced the two features that originate from Ti bonded to F, which were represented by two Voigt functions with tails at 455.9 and 456.9 eV . The corresponding features in the Ti $2p_{1/2}$ XPS spectrum, i.e., at 462.7 and 464.1 eV , is not pronounced, which can be because the background intensity contribution is not always properly represented by a Shirley function.^[6,21]

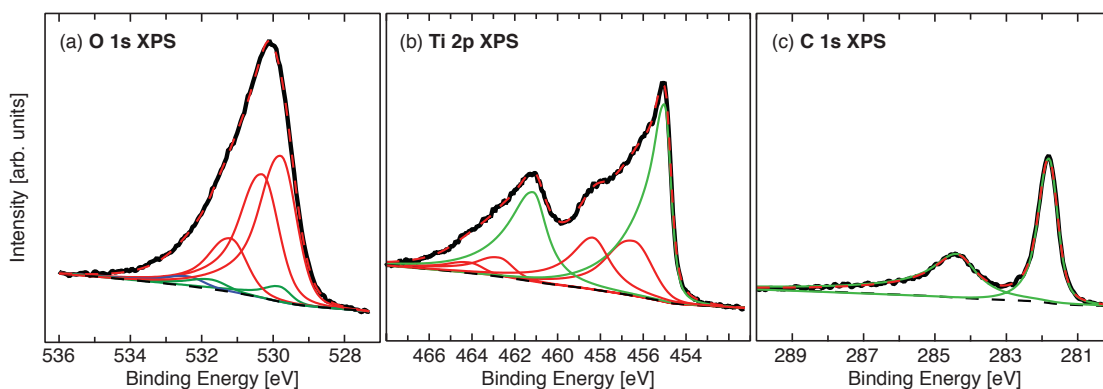


Figure 9. Peak fittings of XPS spectra from the $\text{Ti}_3\text{C}_2\text{T}_x$ film after the H_2 exposure for the core levels (a) O 1s, (b) Ti 2p, and (c) C 1s.

3.2.4. The CO_2 Exposed Sample with Adsorbed H_2

In **Figure 10** the O 1s, Ti 2p, and C 1s XPS spectra after the CO_2 dosing onto the $\text{Ti}_3\text{C}_2\text{T}_x$ sample with adsorbed H show very small intensity variations in the peak fittings compared to the corresponding peak fitting presented in Figure 9. Although some CO_2 might have been adsorbed, the small differences in the XPS spectra are rather reflected by the local variations of coverage at different measurements spots. In fact, the integrated intensities for O 1s and C 1s remain the same before and after the CO_2 dosing, which suggest that no adsorption of CO_2 occurred simply because no sites were available.

A heat treatment removed most of the adsorbed H, which is showed in Figure 5. However, the Ti 2p XPS spectrum in Figure 5(b) shows that there still is some additional intensity at 458.4 eV indicating that some H remains on the $\text{Ti}_3\text{C}_2\text{T}_x$ -surface, which the carbide peak position in the C 1s XPS spectrum corroborates. In addition, Figure 5(a) shows that the O 1s XPS spectrum has different intensity redistribution after the heat treatment.

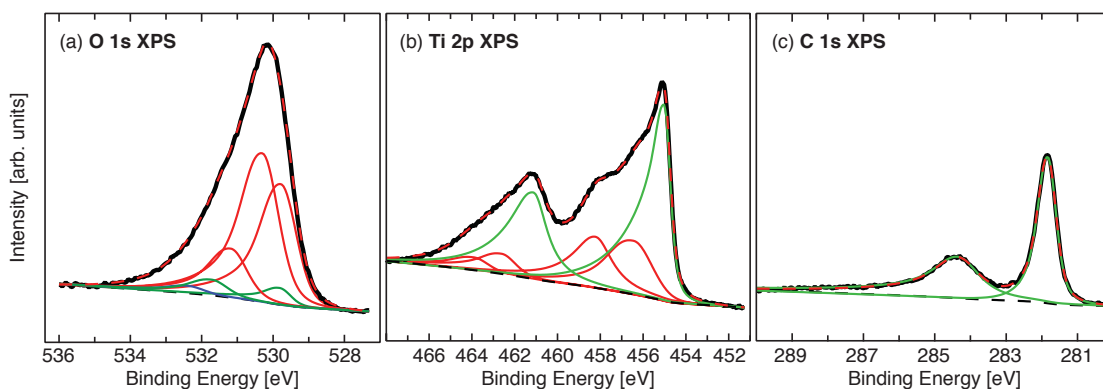


Figure 10. Peak fittings of XPS spectra from the $\text{Ti}_3\text{C}_2\text{T}_x$ film after the $\text{H}_2 + \text{CO}_2$ exposure for the core levels (a) O 1s, (b) Ti 2p, and (c) C 1s.

3.2.5. The CO_2 Exposed Sample

Curve fittings of the O 1s, Ti 2p, and C 1s XPS spectra after the heat treatment that removed most of the adsorbed H are presented in **Figure 11**. The dominating feature in the O 1s XPS spectrum is the one assigned to H_2O on the Ti-Ti bridge-sites. The features at 531.2 and 529.8 eV assigned to O on the fcc-sites and Ti-Ti bridge-sites, respectively, show reduced intensity indicating a loss of atomic O on the $\text{Ti}_3\text{C}_2\text{T}_x$ -surface. Hence, in the heating process the adsorbed H reacted with O and formed H_2O . In the first H addition step an OH-intermediate must be formed, which remained stable long enough for the second H to arrive and react to form H_2O .^[22] However, it cannot be excluded that OH-radicals were desorbed in the heating process before a second H had arrived. A possible reduction of the coverage of O-containing species on the $\text{Ti}_3\text{C}_2\text{T}_x$ -surface would then allow for more diffusion of H_2O from intercalation positions in the bulk of the sample up to the $\text{Ti}_3\text{C}_2\text{T}_x$ -surface.

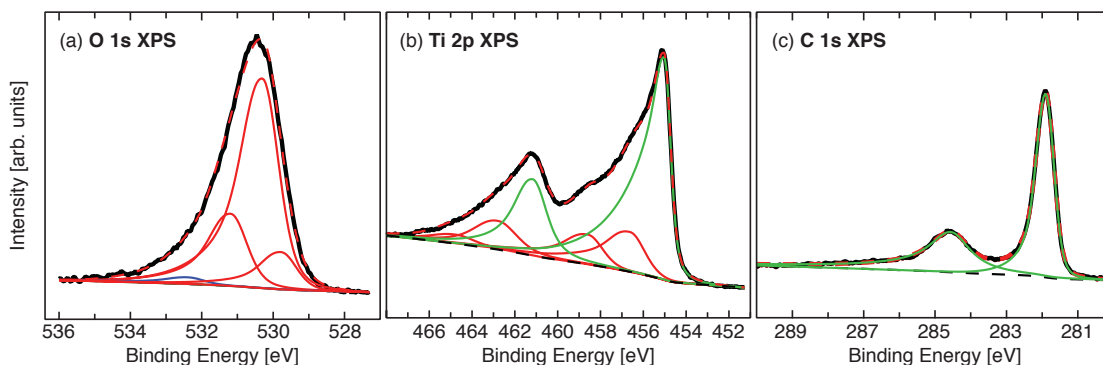


Figure 11. Peak fittings of XPS spectra from the $\text{Ti}_3\text{C}_2\text{T}_x$ film after the second heat treatment for the core levels (a) O 1s, (b) Ti 2p, and (c) C 1s.

Figure 5 showed that with the H removed from the $\text{Ti}_3\text{C}_2\text{T}_x$ -surface it was possible to adsorb CO_2 . **Figure 12** displays the curve fittings of the O 1s, Ti 2p, and C 1s XPS spectra obtained after the CO_2 adsorption. The increased integrated intensity of the O 1s XPS spectrum is a clear evidence of CO_2 adsorption,^[16] although no additional Voigt function was needed in the curve fitting procedure. This supports that the CO_2 contributes with intensity at 530.3 eV,^[16] i.e., at the same binding energy position as H_2O on the Ti-Ti bridge-site. The adsorption site of CO_2 is, however, different compared with H_2O . In addition, the adsorption of CO_2 has forced the O away from the fcc-site and back to the Ti-Ti bridge-site as indicated by the intensity decrease at 531.3 eV and the intensity increase at 529.8 eV. This response has CO_2 adsorption in common with H_2 adsorption (see Figure 8 and 9). Furthermore, the Ti 2p XPS spectrum in Figure 12(b) shows a clear feature at 458.7 eV, which shows similarities as the corresponding feature after the adsorption of H. The similarities shown with CO_2 and H_2 adsorption, and the fact that CO_2 does not adsorb when the $\text{Ti}_3\text{C}_2\text{T}_x$ -surface is covered by H, suggest that both CO_2 and H_2 adsorbs on the Ti on-top sites at the $\text{Ti}_3\text{C}_2\text{T}_x$ -surface, where the latter dissociates.

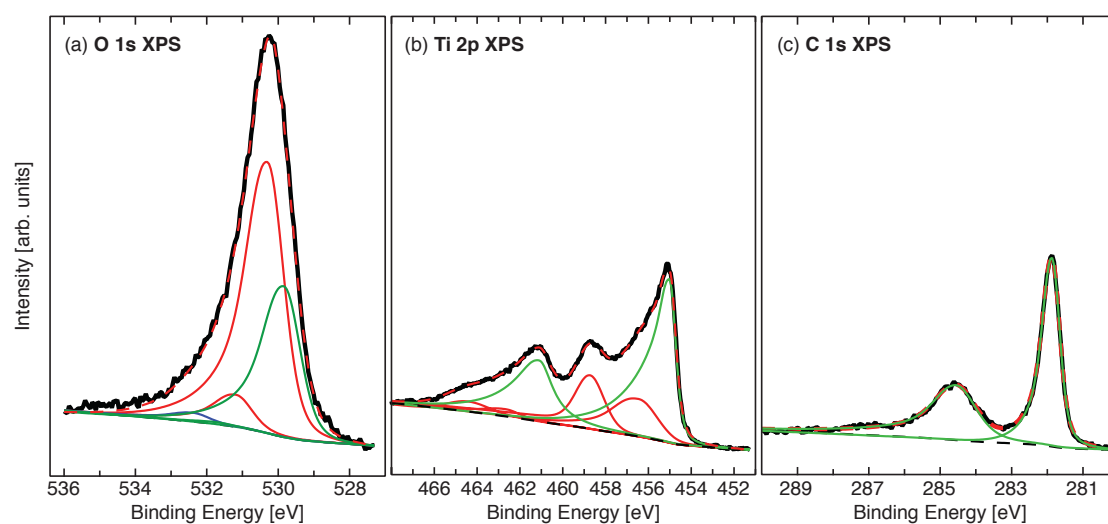


Figure 12. Peak fittings of XPS spectra from the $\text{Ti}_3\text{C}_2\text{T}_x$ film after the CO_2 exposure for the core levels (a) O 1s, (b) Ti 2p, and (c) C 1s.

A recent Ti 1s XANES study showed that the molecular orbitals with Ti 3d and Ti 4p character are very sensitive to termination species and adsorbates.^[9] Hence, the strong interaction between the H, as well as CO_2 , and the molecular orbital available on the

Ti on-top site causes a perturbation of the occupied valence orbitals making the bonding between Ti and O on the fcc-sites less favorable. The perturbation of the occupied valence orbitals will, in addition, change the core hole screening causing a reduction in the kinetic energy of the photoelectrons that are ejected from the probed Ti atoms.^[21] In the Ti 2p XPS spectrum, this is manifested as a redistribution of intensity from 455.0 to 458.7 eV. Similar intensity redistribution, caused by changes in the Ti core hole screening, was observed when Al was deposited on TiN.^[23]

A heat treatment at 650 °C removed the CO₂ from the Ti₃C₂T_x-surface, as shown in **Figure 13**, and the O could then move back to the fcc-sites. Hence, the two dominating features in the O 1s XPS spectrum originate from the O on the fcc-sites at 531.2 eV and the H₂O on the Ti-Ti bridge-sites at 530.3 eV. A small contribution from residual Al₂O₃ at 532.4 eV is also present. The carbide peak in the C 1s XPS spectrum reappear at 282.0 eV indicating that no significant amount of H is present on the Ti₃C₂T_x-surface. However, the curve fitting of the Ti 2p XPS spectrum shows Voigt functions representing Ti 2p_{3/2} features at 456.8 and 458.7 eV and the corresponding Voigt functions at 462.9 and 465.1 eV. The features at 456.8 and 462.9 eV are assigned to Ti bonded to H₂O on a saturated Ti₃C₂T_x-surface. The features at 458.7 and 465.1 eV, which were attributed to the perturbation of the occupied Ti valence orbitals, suggest that some small amount of H might still be present on the Ti on-top sites.

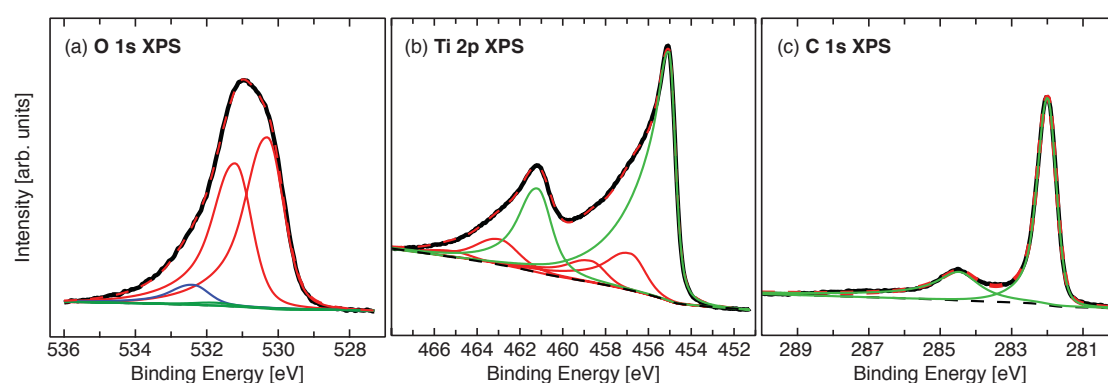


Figure 13. Peak fittings of XPS spectra from the Ti₃C₂T_x film after the third heat treatment for the core levels (a) O 1s, (b) Ti 2p, and (c) C 1s.

3.2.6. The H₂O Exposed Sample

Figure 6 shows that exposing the Ti₃C₂T_x-surface to more H₂O will change the shape of the O 1s XPS spectrum, although without increasing the integrated intensity. The curve fitting displayed in **Figure 14(a)** indicates that the integrated intensity of the H₂O feature at 530.3 eV is intact, which is because of the H₂O saturated Ti-Ti bridge-sites. Instead there is a decrease of the O feature at 531.2 eV and an increase of the O feature at 531.7 eV, where the latter is O on the fcc-sites coadsorbed with another species as shown in previous works.^[3,6] In addition, there is an intensity contribution at 529.8 eV indicating small amounts of O on the Ti-Ti bridge-sites. Furthermore, the intensity increases at 458.7 and 465.1 eV in the Ti 2p XPS spectrum and the small negative shift of the carbide peak, as shown in Figure 6(b) and (c), respectively, suggest that H is present. Since the Ti-Ti bridge-sites are saturated by H₂O there is no other options for the O except remaining at the fcc-sites. The shift from 531.2 to 531.7 eV suggests that the O on the fcc-sites is co-adsorbed with H on the Ti on-top sites. Hence, the O 1s, Ti 2p, and C 1s XPS spectra in Figure 14 reveal a catalytic reaction on the Ti₃C₂T_x-surface where H₂O adsorbs and dissociates. In addition, since the integrated intensity of the O 1s XPS spectrum did not increase upon H₂O exposure, the formed O-containing species must desorb, probably as OH radicals although O₂ cannot be excluded.

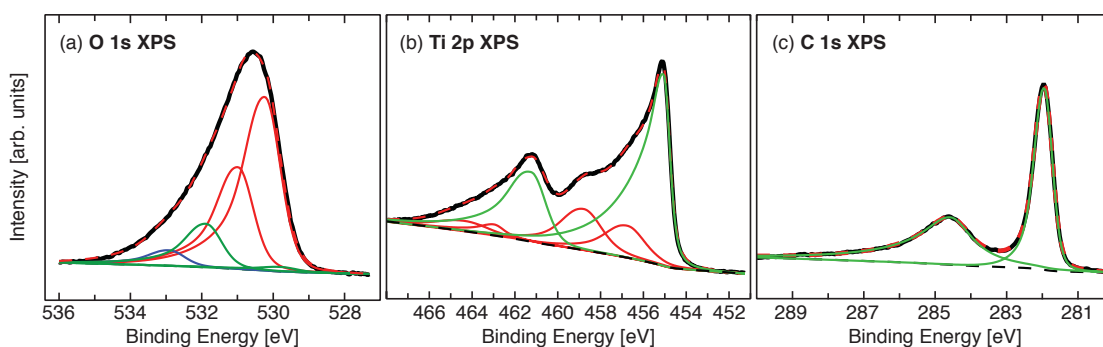


Figure 14. Peak fittings of XPS spectra from the Ti₃C₂T_x film after the H₂O exposure for the core levels (a) O 1s, (b) Ti 2p, and (c) C 1s.

A heat treatment at 700 °C will once again remove most of the adsorbed H and the O 1s, Ti 2p, and C 1s XPS spectra and the curve fittings presented in **Figure 15** are close to identical to the corresponding spectra and curve fittings presented in Figure 13.

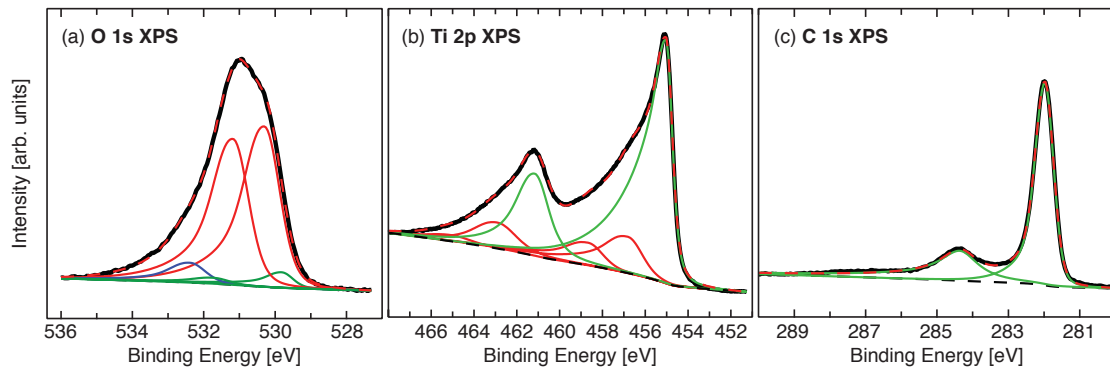


Figure 15. Peak fittings of XPS spectra from the $\text{Ti}_3\text{C}_2\text{T}_x$ film after the fourth heat treatment for the core levels (a) O 1s, (b) Ti 2p, and (c) C 1s.

3.3. No indication of OH on the $\text{Ti}_3\text{C}_2\text{T}_x$ -surface

3.3.1. Valence Band Spectra of the H_2O Exposed Sample

Even though the XPS spectra in Figure 14 suggest the presence of H and, thus, implying H_2O dissociation on the $\text{Ti}_3\text{C}_2\text{T}_x$ -surface, there is no indication of OH in the valence band XPS spectra presented in **Figure 16**. A previous study has shown that OH on the $\text{Ti}_3\text{C}_2\text{T}_x$ -surface would generate a feature around 9 eV in the valence band XPS spectrum.^[5] The three valence band XPS spectra in Figure 16, showing the $\text{Ti}_3\text{C}_2\text{T}_x$ sample before and after H_2O exposure and after heat treatment at 700 °C, are nearly identical and, more importantly, do not show a feature around 9 eV. Hence, there are no indications of OH on the $\text{Ti}_3\text{C}_2\text{T}_x$ -surface.

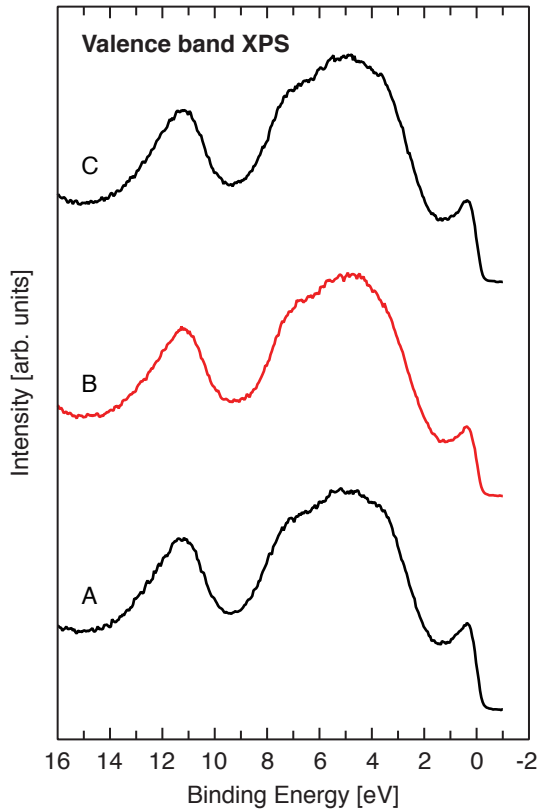


Figure 16. Valence band XPS spectra from the $Ti_3C_2T_x$ film (A) before the H_2O exposure, (B) after the H_2O exposure, and (C) after the fourth heat treatment at $700\text{ }^\circ\text{C}$. Intensity around 5 eV is assigned to T_x on the Ti-Ti bridge-site and intensity around 7 eV is assigned to T_x on the fcc-site. For a comprehensive interpretation of the valence band XPS spectra, see Ref.^[5]

3.3.2. Why OH Might be Observed on $Ti_3C_2T_x$ samples

Considering the numerous publications proposing OH as a termination species, the attempts to prove their presence on the $Ti_3C_2T_x$ -surface are sparse.^[24,25] However, identification of specific species on a surface is a challenge. It requires well-defined samples, i.e. the surface configuration must be known and the sample must be free from impurities and contaminations. Regarding impurities in $Ti_3C_2T_x$, the most common are TiO_2 and Al_2O_3 , which are known to adsorb H_2O that dissociates into OH, see discussion in Ref.^[4-6] In addition, Ti_3AlC_2 is prone to oxidize^[4] and TiO_2 and Al_2O_3 from the pre-etched material can pass through the MXene-forming process and become embedded in the $Ti_3C_2T_x$ -sample.^[26] Any technique that is sensitive toward adsorption species, e.g., XPS, nuclear magnetic resonance (NMR), X-ray absorption spectroscopy (XAS), and electron energy loss spectroscopy (EELS), might therefore

detect OH in the $\text{Ti}_3\text{C}_2\text{T}_x$ -sample, although adsorbed on TiO_2 and/or Al_2O_3 . Even though the $\text{Ti}_3\text{C}_2\text{T}_x$ -sample is free from TiO_2 and Al_2O_3 impurities, precautions must be taken to avoid beam damaging. Many techniques use photons or electrons of high energy and intensity, which might damage the sample. It has, for example, been shown that the use of high-energy electron beam irradiation in an EELS study of $\text{Al}(\text{OH})_3$ was the origin of a feature at 533 eV in the EELS spectrum.^[27] When the energy of the electron beam was reduced the feature at 533 eV did not appear, i.e. beam damaging was avoided. In fact, the EELS study could not identify any feature originating from OH in the EELS data and the authors therefore concluded that O K-edge EELS for the detection of OH is questionable.^[27]

3.4. Comments about the background subtraction

A comparison between the Ti 2p XPS spectrum in Figure 15(b) with the corresponding spectrum in Figure 8(b) is displayed in Figure 6(b). The comparison shows that the spectrum in Figure 15(b) has more intensity around 458.7 eV than the spectrum in Figure 8(b). When there is extra intensity in the Ti $2p_{3/2}$ region the Ti 2p spin orbit splitting requires a corresponding intensity increase in the Ti $2p_{1/2}$ region, although the Ti $2p_{1/2}$ intensity should be half of the Ti $2p_{3/2}$ intensity.^[21] The comparison in Figure 6(b) confirms the increased intensity around 465.1 eV and, thus, consistency information in both Ti $2p_{3/2}$ and Ti $2p_{1/2}$ regions. The curve fittings of the Ti 2p XPS spectra in Figures 13(b) and 15(b) required six Voigt functions for acceptable fitting results, where three are in the Ti $2p_{3/2}$ region and three are in the Ti $2p_{1/2}$ region. However, the intensity ratio between the Ti $2p_{3/2}$ features and the Ti $2p_{1/2}$ features is not consistently 1:2. The reason can be because of that the background intensity, which is unresolved in the Ti 2p region, might deviate from the assumed Shirley function.^[21] However, even if an alternative background subtraction might change the intensity ratio between the Ti $2p_{3/2}$ features and the Ti $2p_{1/2}$ features it would not change the outcome of the curve fittings of the Ti 2p XPS spectra in Figure 9(b)-12(b) and 14(b), where features at 458.7 and 465.1 eV are well resolved in the XPS spectra (in Figure 13(b) and 15(b) the features at 458.7 and 465.1 eV are almost completely reduced in the heat treatment). Hence, although the Ti 2p background might not be represented by a Shirley function completely correct to 100 %, the interpretations based on the curve fittings are valid.

3.5. Summary, Remarks, and Consequences of the Findings

The present study confirms that the termination species on as-prepared $\text{Ti}_3\text{C}_2\text{T}_x$, prepared through wet etching of Ti_3AlC_2 , are F and O on the fcc-sites and on the Ti-Ti bridge-sites, respectively. In addition, a heat treatment significantly reduced the amount of F from the $\text{Ti}_3\text{C}_2\text{T}_x$ -surface and the vacant fcc-sites were subsequently filled by O that have migrated from the Ti-Ti bridge-sites. H_2O was simultaneously diffusing from intercalation positions between the $\text{Ti}_3\text{C}_2\text{T}_x$ -flakes to the newly available Ti-Ti bridge-sites. The process was further assisted by H_2 gas exposure at a moderate temperature increase that efficiently removed the remaining F leading to a saturated $\text{Ti}_3\text{C}_2\text{T}_x$ -surface with O and H_2O as termination species and H as adsorbate. The saturated $\text{Ti}_3\text{C}_2\text{T}_x$ -surface was unable to capture CO_2 . However, removing the H from the $\text{Ti}_3\text{C}_2\text{T}_x$ -surface and the Ti on-top sites became available for CO_2 adsorption. Heat treatments up to $700\text{ }^\circ\text{C}$ removes adsorbates (H and CO_2) but could not remove H_2O from the $\text{Ti}_3\text{C}_2\text{T}_x$ -surface. In fact, H_2O is more strongly bonded to the $\text{Ti}_3\text{C}_2\text{T}_x$ -surface than H. H_2O can therefore be considered being a termination species sitting on the Ti-Ti bridge-site. Furthermore, additional H_2O exposure to a $\text{Ti}_3\text{C}_2\text{T}_x$ -surface with termination species in a saturated condition shows water-splitting quality. Even so, while the H coverage increases because of H_2O dissociation the amount of O-termination remained unchanged.

Consequently, $\text{Ti}_3\text{C}_2\text{T}_x$ as a CO_2 capturing material requires a preparation method that avoids intercalation of H_2O between 2D $\text{Ti}_3\text{C}_2\text{T}_x$ -flakes, because intercalated H_2O between 2D $\text{Ti}_3\text{C}_2\text{T}_x$ -flakes will become a source of $\text{Ti}_3\text{C}_2\text{T}_x$ -surface poisoning for the CO_2 adsorption process. In addition, $\text{Ti}_3\text{C}_2\text{T}_x$ as a CO_2 capturing material requires a moisture free environment. An additional implication with H_2O as a termination species on the Ti-Ti bridge-site is that it might affect the intercalation of positive ions, such as Li^+ and Na^+ . As discussed in a previous publication,^[5] O on the Ti-Ti bridge-site might act as anchor points in intercalation processes. The two electron lone pairs on the O are lobes with negative charge that are pointing out from the $\text{Ti}_3\text{C}_2\text{T}_x$ -surface and will therefore attract positively charged species, such as positive ions and the positive end of dipolar molecules. The present study has showed that a $\text{Ti}_3\text{C}_2\text{T}_x$ -sample can be intercalated with H_2O , which probably bonds to the O on the Ti-Ti bridge-sites through hydrogen bonding. Hence, O in the Ti-Ti bridge-site might be a prerequisite for the intercalation process of Li^+ and/or Na^+ , which probably have

solvation spheres of H₂O that bond to the O on the Ti-Ti bridge-sites through hydrogen bonding. When the O on the Ti-Ti bridge-sites are replaced by H₂O, with the hydrogen atoms pointing out from the Ti₃C₂T_x-surface, the H₂O in the solvation spheres of positive ions will be repelled because the hydrogen atoms of the H₂O in the solvation sphere will be pointing outwards. H₂O on the Ti-Ti bridge-sites will, on the other hand, attract negative ions or the negative end of the dipolar molecules. Hence, the present XPS study suggests that when Ti₃C₂T_x is utilized as an ion storage material the Ti-Ti bridge-site must be occupied by O for positive ions and H₂O for negative ions.

The curve fittings of the XPS spectra were performed according to first principles thinking, as presented in a previous publication.⁶ The peak positions of the Voigt functions used in the curve fittings correspond to the binding energies of the Ti and C in the Ti₃C₂-layer, the terminating species F, O, and H₂O, and the adsorbate CO₂. The obtained binding energies are presented in **Table 1**.

One ion in particular that Ti₃C₂T_x seems to be able to store is H⁺ and that at room temperature and low pressure. The H₂ molecule dissociates on the Ti₃C₂T_x-surface and the adsorbed H lend its electron to the C layers in the Ti₃C₂T_x crystal structure. The hydrogen can later on be released from the Ti₃C₂T_x at a moderate temperature increase, restoring the Ti₃C₂T_x to the same condition prior the H₂ gas exposure (although the process requires an H₂O free environment).

The present study has revealed a new termination species but also new information utilizing Ti₃C₂T_x as ion storage material, CO₂ capture material, and a H₂O splitting material. The obtained information demonstrates the requirements needed for particular application and, thus, guidance toward correct surface conditions when Ti₃C₂T_x is activated in various future energy storage, CO₂ capture, or energy converting devices.

Table 1. Binding energies for core level electrons in $\text{Ti}_3\text{C}_2\text{T}_x$.

Region	Binding Energy [eV]	Designation	
C 1s	281.8	$\text{Ti}_3\text{C}_2\text{T}_x$ with adsorbed H	
	282.0	$\text{Ti}_3\text{C}_2\text{T}_x$	
	284.2	multilayer graphite-like carbon	
	284.5	graphite-like carbon on $\text{Ti}_3\text{C}_2\text{T}_x$	
	284.6	CO_2 on $\text{Ti}_3\text{C}_2\text{T}_x$	
	Ti 2p _{3/2}	455.0	$\text{Ti}_3\text{C}_2\text{T}_x$ with O termination
455.9		$\text{Ti}_3\text{C}_2\text{T}_x$ with F and O termination	
456.6		$\text{Ti}_3\text{C}_2\text{T}_x$ with O and H_2O termination	
456.9		$\text{Ti}_3\text{C}_2\text{T}_x$ with F termination	
458.3		$\text{Ti}_3\text{C}_2\text{T}_x$ with adsorbed H on Ti on-top site	
458.7		$\text{Ti}_3\text{C}_2\text{T}_x$ with adsorbed CO_2 on Ti on-top site	
Ti 2p _{1/2}		461.2	$\text{Ti}_3\text{C}_2\text{T}_x$ with O termination
		462.3	$\text{Ti}_3\text{C}_2\text{T}_x$ with F and O termination
	462.8	$\text{Ti}_3\text{C}_2\text{T}_x$ with O and H_2O termination	
	463.3	$\text{Ti}_3\text{C}_2\text{T}_x$ with F termination	
	464.1	$\text{Ti}_3\text{C}_2\text{T}_x$ with adsorbed H on Ti on-top site	
	464.8	$\text{Ti}_3\text{C}_2\text{T}_x$ with adsorbed CO_2 on Ti on-top site	
	O 1s	529.8	O termination on Ti-Ti bridge-site
530.3		H_2O termination on Ti-Ti bridge-site	
530.3		CO_2 adsorbed on Ti on-top site	
531.2		O termination on fcc-sites in domains with only O	
531.7		O termination on fcc-sites in domains with F	
532.4		Residual Al_2O_3	
F 1s		684.4	F termination on fcc-sites in domains with only F
	685.2	F termination on fcc-sites in domains with O	

4. Conclusions

From the XPS study of the $\text{Ti}_3\text{C}_2\text{T}_x$ freestanding film we conclude that the as-prepared sample was almost completely saturated by F on the fcc-sites and almost completely saturated by O on the Ti-Ti bridge-sites. Removing F from the $\text{Ti}_3\text{C}_2\text{T}_x$ -surface through heat treatments and/or reaction with H enabled O-migration from the Ti-Ti bridge-sites to the fcc-sites that became vacant when the F were removed. The vacant Ti-Ti bridge-sites could then be occupied by H_2O that have diffused from intercalated positions between $\text{Ti}_3\text{C}_2\text{T}_x$ flakes to the $\text{Ti}_3\text{C}_2\text{T}_x$ -surface during the heat treatment. The H_2O remained on the Ti-Ti bridge-sites even after several sample heat treatments at temperatures up to 700 °C. Hence, a new termination species is identified.

Hydrogen adsorbs on the $\text{Ti}_3\text{C}_2\text{T}_x$ -surface and modification in the Ti 2p spectrum indicates that the Ti on-top site on the $\text{Ti}_3\text{C}_2\text{T}_x$ -surface is an H absorption site. Other adsorption sites cannot be excluded, although the O and H_2O that were present as termination species might have limited the options in this study. Nevertheless, the carbide peak in the C 1s XPS spectrum shows that the two C layers in the $\text{Ti}_3\text{C}_2\text{T}_x$ crystal structure gained charge when H was adsorbed.

With the $\text{Ti}_3\text{C}_2\text{T}_x$ -surface completely covered by O, H_2O , and H there are no sites available for CO_2 adsorption. Some amount of CO_2 can, on the other hand, be adsorbed on the Ti on-top sites then the H is absent. However, in this study the CO_2 was adsorbed when O and H_2O were present as termination species and other adsorption sites might therefore be possible when the Ti_3C_2 -surface is free from termination species.

The adsorption of H and/or CO_2 on the Ti on-top site perturbs the molecular orbitals enough to make the fcc-site unfavorable for the O occupation. The O will then migrate back to the Ti-Ti bridge-sites. The Ti-Ti bridge-sites will then be saturated by O and H_2O , which prevents adsorption of H and/or CO_2 on the Ti-Ti bridge-sites. Hence, to maximize the CO_2 adsorption, e.g., in an application as a carbon-capturing device, the Ti_3C_2 -surface must be termination free and without the possibility for intercalated H_2O to diffuse to the surface.

A $\text{Ti}_3\text{C}_2\text{T}_x$ -surface, saturated with O and H_2O termination, has the ability to split water. Even so, there are no signs of adsorbed OH on the $\text{Ti}_3\text{C}_2\text{T}_x$ -surface. This observation suggests desorption of OH-radicals or a complete dissociation followed by an O_2 formation and desorption.

Acknowledgements

We thank Dr Joseph Halim at Linköping University for preparing the sample and Dr Mikko-Heikki Mikkela and Dr Margit Andersson for experimental support at the MAX IV Laboratory. Research conducted at MAX IV, a Swedish national user facility, is supported by the Swedish Research council under contract 2018-07152, the Swedish Governmental Agency for Innovation Systems under Contract 2018-04969, and Formas under Contract 2019-02496. We also thank the Swedish Government Strategic Research Area in Materials Science on Functional Materials at Linköping University (Faculty Grant SFO-Mat-LiU No. 2009 00971). M. M. acknowledges financial support from the Swedish Energy Research (Grant No. 43606-1) and the Carl Tryggers Foundation (CTS23:2746, CTS20:272, CTS16:303, CTS14:310).

References

- [1] Y. Xie, Y. Dall'Agnese, N. Naguib, Y. Gogotsi, M. W. Barsoum, H. L. Zhuang, P. R. Kent, *ACS Nano* **2014**, *8*, 9606-9615.
- [2] M. Naguib, V. N. Mochalin, M. W. Barsoum, Y. Gogotsi, *Adv. Mater.* **2014**, *26*, 992-1005.
- [3] I. Persson, L.-Å. Näslund, J. Halim, M. W. Barsoum, V. Darakchieva, J. Palisaitis, J. Rosen, P. O. Å Persson, *2D Mater.* **2018**, *5*, 015002.
- [4] L.-Å. Näslund, P. O. Å Persson, J. Rosen, *J. Phys. Chem. C* **2020**, *124*, 27732-27742.
- [5] L.-Å. Näslund, M.-H. Mikkela, E. Kokkonen, M. Magnuson, *2D Mater.* **2021**, *8*, 045026.
- [6] L.-Å. Näslund, I. Persson, *Appl. Surf. Sci.* **2022**, *593*, 153442.
- [7] P. O. Å Persson, J. Rosen, *Curr. Opin. Solid State Mater. Sci.* **2019**, *23*, 100774.
- [8] I. Persson, J. Halim, H. Lind, T. W. Hansen, J. B. Wagner, L.-Å. Näslund, V. Darakchieva, J. Palisaitis, J. Rosen, P. O. Å Persson, *Adv. Mater.* **2019**, *31*, 1805472.
- [9] L.-Å. Näslund, M. Magnuson, *2D Mater.* **2023**, *10*, 035024.

- [10] S. Urpelainen, C. Sâthe, W. Grizoll, M. Agâker, A. R. Head, M. Andersson, S.-W. Huang, B. N. Jensen, E. Wallén, H. Tarawneh, R. Sankari, R. Nyholm, M. Lindberg, P. Sjöblom, N. Johansson, B. N. Reinecke, M. A. Arman, L. R. Merte, J. Knudsen, J. Schnadt, J. N. Andersen, F. Hennies, *J. Synchrotron Rad.* **2017**, *24*, 344-353.
- [11] E. Kokkonen, F. L. da Silva, M.-H. Mikkela, N. Johansson, S.-W. Huang, J.-M. Lee, M. Andersson, A. Bartalesi, B. N. Reinecke, Karsten Handrup, H. Tarawneh, R. Sankari, J. Knudsen, J. Schnadt, C. Sâthe, S. Urpelainen, *J. Synchrotron Rad.* **2021**, *28*, 588-601.
- [12] M. H. Engelhard, D. R. Baer, A. Herrera-Gomez, P. M. A. Sherwood, *J. Vac. Sci. Technol. A* **2020**, *38*, 063203.
- [13] WaveMetrics, Igor Pro version 6.22A, <https://www.wavemetrics.com/>, accessed: February, **2011**.
- [14] V. Natu, M. Benchakar, C. Canaff, A. Habrioux, S. Célérier, M. W. Barsoum, *Matter* **2021**, *4*, 1224-1251.
- [15] M. D. Tucker, Z. Czigány, E. Broitman, L.-Å. Näslund, L. Hultman, J. Rosen, *J. Appl. Phys.* **2014**, *115*, 144312.
- [16] C. Kunkel, F. Viñes, P. J. Ramírez, J. A. Rodriguez, F. Illas, *J. Phys. Chem. C* **2019**, *123*, 7567–7576.
- [17] D. R. Cousens, B. J. Wood, J. Q. Wang, A. Atrens, *Surf. Interface Anal.* **2000**, *29*, 23–32.
- [18] A. V. Shchukarev, D. V. Korolkov, *Cent. Eur. J. Chem.* **2004**, *2*, 347-362.
- [19] N. Cai, G. Zhou, K. Müller, D. E. Starr, *J. Phys. Chem. C* **2013**, *117*, 172–178.
- [20] O. Björneholm, A. Nilsson, H. Tillborg, P. Bennich, A. Sandell, B. Hernnk, C. Puglia, N. Mårtensson, *Surf. Sci.* **1994**, *315*, L983-L989.
- [21] S. Hüfner, *Photoelectron Spectroscopy: Principles and Applications*, third ed., Springer-Verlag, Berlin, Germany **2010**.
- [22] L.-Å. Näslund, *Surf. Sci.* **2013**, *618*, 42–48.
- [23] G. Greczynski, I. Petrov, J. E. Greene, Hultman, *J. Vac. Sci. Technol. A* **2015**, *33*, 05E101.
- [24] J. Halim, K. M. Cook, M.; Naguib, P. Eklund, Y. Gogotsi, J. Rosen, M. W. Barsoum, *Appl. Surf. Sci.* **2016**, *362*, 406–417.
- [25] M. A. Hope, A. C. Forse, K. J. Griffith, M. R. Lukatskaya, M. Ghidui, Y. Gogotsi, C. P. Grey, *Phys. Chem. Chem. Phys.* **2016**, *18*, 5099–5102.

- [26] M. Magnuson, J. Halim, L.-Å. Näslund, *J. Electron Spectrosc.* **2018**, 224, 27–32.
- [27] N. Jiang, J. C. H. Spence, *Ultramicroscopy* **2011**, 111, 860-864.

Adsorption of Gases on $\text{Ti}_3\text{C}_2\text{T}_x$ MXene: Implications from X-ray Photoelectron Spectroscopy

X-ray photoelectron spectroscopy shows adsorption of H_2 , CO_2 , and H_2O on the $\text{Ti}_3\text{C}_2\text{T}_x$ -surface. The results indicate that hydrogen adsorbs on the Ti on-top site, H_2O bonds strongly to the Ti-Ti bridge-sites, and an H_2O terminated $\text{Ti}_3\text{C}_2\text{T}_x$ -surface restricts the CO_2 adsorption to the Ti on-top sites. The study shows no signs of adsorbed OH on the $\text{Ti}_3\text{C}_2\text{T}_x$ -surface.

L.-Å. Näslund,* E. Kokkonen, M. Magnuson

